Title

THE INCLUSIVE REACTION p + p -> n- + ANYTHING AT 6.6 GeV/c COMPARED TO HIGHER ENERGIES

Author

Gellert, Eugene.

Publication Date

1972-02-01

Presented at International Conference
on Inclusive Reactions, Davis,
California, February 4-5, 1972

LBL-784
Preprint

THE INCLUSIVE REACTION $p + p \rightarrow \pi^- +$ ANYTHING AT 6.6 GeV/c COMPARED TO HIGHER ENERGIES

Eugene Gellert

February 5, 1972

AEC Contract No. W-7405-eng-48

DISCLAIMER

THE INCLUSIVE REACTION $pp \to \pi^-$ + anything AT 6.6 GeV/c COMPARED TO HIGHER ENERGIES

Eugene Gellert
Lawrence Berkeley Laboratory, University of California
Berkeley, California 94720

February 5, 1972

ABSTRACT

The π^- distribution from $pp \to \pi^-$ + anything at 6.6 GeV/c is studied and compared to higher energies. It is found that for $p_\perp < 0.6$ GeV/c and Feynman's $x < -0.4$, the laboratory differential cross section $d^2\sigma/dp_\perp dp_\parallel$ is independent of energy. The structure function $\rho(x, p_\perp, s) = Ed^3\sigma/dp^3$ is found not to be energy independent and is found not to be factorizable into functions of transverse and longitudinal momentum.

I. INTRODUCTION

From mid-August to November 1, 1965, we exposed the Alvarez 72-inch liquid-hydrogen bubble chamber to 6.6 and 5.4 GeV/c protons from the Bevatron external-proton-beam. A description of the experimental set up can be found elsewhere.[1]

In this paper we confine our attention to π^- production. Proton production was discussed in an earlier paper.[2]

We merely present our results with very little further discussion of the general subject of inclusive reactions, in order not to duplicate the many other papers presented at this conference.

II. DATA ANALYSIS

Although a total of 493 000 pictures were taken at both energies, <u>the results reported here represent a subsample of the pictures taken at 6.6 GeV/c</u>. Because we are looking at the reaction $p + p \to$

π^- + anything, only the 4 and 6-prong events are examined. (The 8, 10, and higher-prong cross sections are negligable at 6.6 GeV/c.) The film was measured on the Franckensteins (~$\frac{1}{2}$ the

Table I. The 4 and 6-prong sample

	No. of pictures scanned & measured	No. of events passing fiducial criteria
4-prongs	93 000	25 274
6-prongs	153 000	2 747

events), the S.M.P's (1/10 the events), and the 40cm-radius Spiral Reader I (~4/10 the events), and the measured events were processed through the kinematic-reconstruction program TVGP and the fitting program SQUAW.[3]

III. RESULTS

The results presented here are abstracted from a longer paper currently being prepared.

A. Cross Sections

The cross sections determined by this experiment are listed below.

Table II. Cross Sections

	Nominal momentum	
	5.4 GeV/c	6.6 GeV/c
Total cross section (mb)[a]		38.9 ± 1.2
Total inelastic-cross-section (mb)[b]		28.8 ± 0.8
Topological cross sections (mb)		
2-prongs[c]		
elastic		10.16 ± 0.55

Table II (continued)

inelastic		16.83 ± 0.70
total		27.0 ± 1.1
4-prongs[d]		10.50 ± 0.46
6-prongs[e]		0.727 ± 0.094
8-prongs[f]		0.022 ± 0.008
10-prongs[f]		0.009 ± 0.005
Strange particles[g]	0.624	0.674
<u>Cross-section ratios</u>		
$\sigma_{6\text{-prong}}/\sigma_{4\text{-prong}}$[e]		0.0692 ± 0.0084
$\sigma_{8\text{-prong}}/\sigma_{4\text{-prong}}$[f]		0.0021 ± 0.0008
$\sigma_{10\text{-prong}}/\sigma_{4\text{-prong}}$[f]		0.0009 ± 0.0005

a. the sum of all the topological cross sections listed below

b. the sum of all the topological cross sections listed below except the elastic cross section

c. calculated from the results reported in ref. 1a

d. from ref. 1a

e. The error in $\sigma_{6\text{-prong}}/\sigma_{4\text{-prong}}$ is almost entirely the result of uncertainties in scanning efficiency, not the statistical error in the number of events scanned. The 6-prong cross section was obtained by multiplying this ratio by the 4-prong cross section. The error in the 6-prong cross section thus obtained is due almost entirely to the error in this ratio.

f. The error presented is essentially the result of the statistical error of 7 and 3 events (for the 8-prongs and 10-prongs, respectively); no attempt was made to estimate the scanning biases.

g. Arthur Barry Wicklund (Argonne National Lab.), personal communication, 1968

B. Definitions

Throughout this paper "*"'d quantities represent variables evaluated in the center-of-momentum of the incident beam and target. If the possibility of confusion arises, unstarred quantities always represent variables to be evaluated in the laboratory system.

The Lorentz invariant cross section or structure function is defined by

$$\rho = E d^3\sigma / dp^3, \qquad (1)$$

where E and p are the energy and momentum of the π^- in any Lorentz frame. We shall define Feynman's x by

$$x = p^*_{\parallel}/p^*_{max} \qquad (2)$$

and the rapidity, y, by

$$y = \tanh^{-1}(p_{\parallel}/E) \qquad (3)$$

C. Comparisons with Higher Energy Experiments in the Laboratory System

Dennis Smith showed that for proton-proton collisions from 13 to 28.5 GeV/c, the hypothesis of limiting distributions is correct for the target fragmentation region, that is $d^2\sigma/dp_{\perp}dp_{\parallel}$(lab) is independent of the overall energy of the reaction.[4] He therefore only tabulates $d^2\sigma/dp_{\perp}dp_{\parallel}$ averaged over all his energies, rather than for each energy seperately. We compare our 6.6 GeV/c data with his (fig. 1). For seven equal intervals in $p_{\perp}$, from 0.0 to 0.7 GeV/c, we plot $d^2\sigma/dp_{\perp}dp_{\parallel}$ for π^- versus $p_{\parallel}$(lab) for both experiments.[†,‡] Various vertical lines are drawn on fig. 1 in order to show the relation

---

† However, before making this plot, we must first divide the values given by D. Smith (in Table VII of ref. 4) by two. This is necessary because he has actually tabulated $d^2\sigma/dp_{\perp}dp_{\parallel}$(beam rest frame) + $d^2\sigma/dp_{\perp}dp_{\parallel}$(lab) in order to improve his statistics, just as we do, but he has not divided the sum by two, as we do.[5]

‡ We plot $d^2\sigma/dp_{\perp}dp_{\parallel}$ rather than ρ only because D. Smith chose to do this. From the definition of ρ it is immediatly obvious that $d^2\sigma/dp_{\perp}dp_{\parallel}$(lab) can be independent of the incident particle energy if and only if $\rho(p_{\perp},p_{\parallel},s) = \rho(p_{\perp},p_{\parallel})$. It is only when we compare distributions at different $p_{\parallel}$(or $p_{\perp}$), for example, when we compare the structure function at the same $p_{\perp}$ and x for different values of s, that it is important to use ρ rather than the differential cross section, in order to eliminate an uninteresting phase space factor.

between the C.M. and lab. systems for each $p_\perp$ interval. The rightmost pair of broken lines on each plot are the minimum and maximum values of $p_{//}$(lab) for $\underline{x} = 0$, for D. Smith's data, and the rightmost pair of solid lines are the same thing for our 6.6 GeV/c data. Going left, the next set of lines correspond to the minimum and maximum values of $p_{//}$(lab) for $\underline{x} = -0.5$. Clearly $p_{//}$(lab) changes slowly with $\underline{s}$, for constant $\underline{x}$, in this region of $\underline{x}$. Finally, the two leftmost pairs of lines indicate the minimum value of $p_{//}$(lab) possible, over the range of $p_\perp$ and $\underline{s}$ in question.

We observe that for $\underline{x} \lesssim -0.4$, our data is in excellent agreement with D. Smith's, except for our highest $p_\perp$ interval (for which $p_\perp = \frac{1}{2}p_{\perp,max}$; $p_{\perp,max} = 1.35$ GeV/c). However, our data falls below Smith's for $\underline{x} \gtrsim -0.4$. There is also some disagreement at the very lowest $p_{//}$, where the differential cross section for our energy is always less than for higher energy.†

A similar comparison is made with the 12.4 GeV/c counter data of Akerlof <u>et al</u>. (fig. 2a).[6] The upper two curves (which correspond to fig. 1c) show agreement at small values of $p_{//}$(lab), while the next two curves (which correspond to fig. 1a) do not quite agree, even for small $p_{//}$; the 6.6 curve is always below the 12.4 curve. The comparison with Akerlof <u>et al</u>. and the comparison with D. Smith are therefore in agreement.

D. Comparison with Higher Energy in the Overall Center-of-Momentum System

† We do note, however, that the π^- can have more backward momentum for higher energy reactions. Also, we have not corrected for the fact that our most backward bin in $p_{//}$ is partly below the kinematic limit, while that for the higher energy experiment is not.

Next, we investigate the properties of the central region, i.e. the region of small $|x|$. Because the value of $p_{//}$(lab) for x = 0 depends strongly on s, the lab. system is not appropiate for the study of this region, and we therefore compare data in the C.M. system, chosing Feynman's-x and $p_\perp$ as our variables.[8] Because the data tabulated by D. Smith is averaged over a variety of energies, it is not possible, strictly speaking, to transform it to the C.M. system, and we therefore confine our attention to the 12.4 GeV/c counter data (fig. 2b).†

We bin our 6.6 GeV/c data so that the center of each of our bins is equal in both x and $p_\perp^2$ to one of Akerlof's points.‡ Clearly, there is no agreement for $x \gtrsim 0$, where $\rho(12.4) \approx 2\rho(6.6)$. We note that this same relation holds between π^- production-cross-sections, i.e. $\sigma_{\pi^-}(12.4) = 1.83\sigma_{\pi^-}(6.6)$. In order to try to understand this disagreement at small x, we plot $U = (1/\sigma_{\pi^-}(s))d^2\sigma/dp_\perp^2 dp_{//}^*$ vs. $p_{//}^*$ (fig. 2c). There is fair agreement for not too large values of $p_{//}^*$, especially for the lowest value of $p_\perp^2$ (0.21 $(\mathrm{GeV/c})^2$). Because most π^-'s that contribute to σ_{π^-} come from the region $p_\perp^2 < 0.21$ $(\mathrm{GeV/c})^2$, independence of U with respect to x at $p_\perp^2 = 0.21$ makes it almost certain that U is also independent of s for $p_\perp^2 < 0.21$. Therefore, we may write

$$d^2\sigma/dp_\perp^2 dp_{\shortparallel}^* = g(p_\perp^2, p_{\shortparallel}^*)h(s)$$

or, equivalently

$$\rho(p_{\shortparallel}^*, p_\perp, s) = g'(p_\perp, p_{\shortparallel}^*)h(s),$$

for $p_{\shortparallel}^*$ and $p_\perp$ not too large.

Returning to our consideration of the $p_\perp^2 = 0.21$ $(\mathrm{GeV/c})^2$ points of

---

†Actually, in as much as there appears to be a limiting distribution in the target fragmentation region, we could assume that D. Smith's quoted distribution is correct for each and every beam energy of his experiment, and we therefore could make a separate Lorentz transformation of his distribution for each such energy. Because we do have Akerlof's points available, we chose not to do this, however.

‡For this reason, we do not show our data in the half bin nearest x = 0. However, fig. 6a does show that nothing unusual happens in this region.

fig. 2b, although at $x \approx 0$ we have $\rho(12.4) \approx 2\rho(6.6)$, the two curves become identical in the region from x = 0.34 to 0.49, after which $\rho(12.4)$ is less than $\rho(6.6)$. Even neglecting our anomalously high data point at $\underline{x} = 0.54$, this disagreement at high $\underline{x}$ is clearly beyond statistical error; for x = 0.73, we have $\rho(12.4) = \frac{1}{4}\rho(6.6)$!

It is instructive to contrast this disagreement at large $\underline{x}$ with the previously noted agreement at small and backward $p_{\parallel}$(lab). Each and every data point of fig. 2a can be identified with a unique data point of fig. 2b, because each data point of fig. 2a is obtained by transforming a fig. 2b data point. A broken line on each plot connects points having $\underline{x} = 0.489$. It is apparent that for $p_{\perp}^2 = 0.21$ (GeV/c)^2 and $x \approx -0.5$, Akerlof et al.'s points are shifted about one bin below our points in $p_{\parallel}$(lab), increasing to about $1\frac{1}{2}$ bins for Akerlof's last point at $\underline{x} = -0.73$. We therefore conclude that, so long as ρ is not flat with respect to $\underline{x}$, it is not possible to have agreement of different energy curves in both $\underline{x}$ and $p_{\parallel}$(lab), simply because of the properties of the Lorentz transformation. The fact that we have agreement in the lab. system necessarily means that we cannot have agreement in the $\underline{x}$ system.[†]

For $p_{\perp}^2 < 0.21$ (GeV/c)^2 this shift toward lower $p_{\parallel}$(lab) for increasing $\underline{s}$ would be even greater, and, furthermore, if we compared our 6.6 GeV/c experiment with an experiment even higher in $\underline{s}$ than Akerlof's, this shift would be still greater. Therefore, a comparison of our experiment with D. Smith's (P_{beam} = 13 to 28.5 GeV/c) for low $p_{\perp}$, for which, as we have already seen, there is agreement for small $p_{\parallel}$(lab), should show even more disagreement at high $\underline{x}$ than does our comparison with Akerlof.

In fig. 3d, the same set of data points are plotted, this time against the lab. rapidity, $y = \tanh^{-1}\left[p_{\parallel}(\text{lab})/E(\text{lab})\right]$. Because we are still in the lab., the curves will agree and disagree for exactly the same points as on fig. 2a. To make a plot of ρ vs. $y-y_{min}$, we would

[†]But see Addendum for a further discussion of ρ vs. $\underline{x}$

shift each set of points rigidly to the right, but Akerlof et al.'s points would be shifted further right than ours, because y_{min} is less for their points. We indicate the relative shift of their points by attaching a rightward pointing arrow to some of them. For the lowest $p_\perp$, the curves would have the same crossover property as do the ρ vs. x curves.

E. One Dimensional Distributions

Various longitudinal distributions for the 4-prongs, 6-prongs, and combined 4 and 6-prong sample are presented (fig. 3). First, we plot $F(x,s) = \int_0^{p_\perp^2 \max} \rho(x,p_\perp^2,s)dp_\perp^2$ vs. x (fig. 3a). The 6-prongs contribute only to the center of the plot. The error bars attached to the data points represent the statistical errors only. The error bar at a is the 6-prong normalization error, and the error bar at b (which is smaller than the symbol to which it is attached) is the maximum contribution that this error can make to the error of the combined sample. We also plot $d\sigma/dx$ vs. x (fig. 3b), the laboratory differential cross section (fig. 3c), and the integrated structure function $B(y,s) = \int_0^{p_\perp^2 \max} \rho(y,p_\perp^2,s)dp_\perp^2$ vs. the lab. rapidity, y (fig. 3d).

Further, we plot π^- distributions (F vs. x and G vs. $p_\perp^2$) according to the number of pions produced (fig. 4). The various reactions giving different numbers of pions are listed below. In order to more easily see the fraction of F and G contributed by each of the various final states, we also plot F/F_{total} and G/G_{total} (fig. 5). Figures 5a and 5d show that the two 3π final states are clearly identical in shape and magnitude, except for small x or small $p_\perp^2$, where the final state containing the neutron is larger. There is copious $\Delta^-(1238)$ production in this final state however; about 50% of the π^-'s come from the

Table III. Contributions of reactions having 2, 3, and $\geq 4\pi$'s to the inclusive reaction $p + p \rightarrow \pi^- +$ anything at 6.6 GeV/c.

	Reaction	π^- Production Cross Section[a]
2π's	$pp \rightarrow pp\pi^+\pi^-$	2.90 ± 0.12 mb[b]
3π's	$pp \rightarrow pp\pi^+\pi^-\pi^0$	2.29 ± 0.09 mb[b]
	$pn\pi^+\pi^+\pi^-$	2.77 ± 0.11 mb[b]
$\geq 4\pi$'s	$pp \rightarrow pp\pi^+\pi^-mm$ ($mm \geq 2\pi^0$'s) $p\pi^+\pi^+\pi^-mm$ ($mm \geq n+\pi^0$) $\pi^+\pi^+\pi^+\pi^-mm$ ($mm \geq 2n$'s)	2.36 ± 0.10 mb[b,c]
	all 6-prongs	1.45 ± 0.18 mb

a. The π^- production cross section, σ_{π^-}, for a class of events is equal to $n_{\pi^-}\sigma$, where n_{π^-} is the number of π^-'s per event, and σ is the cross section for the class of events in question.

b. Statistical error and normalization error only — does not include systematic errors of up to 10% from wrong fits.

c. We have neglected the small amount of $d\pi^+\pi^+\pi^-$ final states in our plots of the 3π sample. The total 4-prong cross section includes deuteron final states.

$\Delta^-(1238)$.[7] We have not yet investigated whether the excess events at small $\underline{x}$ do, in fact, come from the $\Delta^-(1238)$.

Next, we investigate the different reactions having four or more π's in the final state. Because, aside from a small number of deuteron events, the 4-prong final states in this class all produce unconstrained fits, we do not consider them separately, but instead, we only compare them with the 6-prongs, which — of course — all have four or more π's. Because σ_{π^-}(4-prongs, $\geq 4\pi$'s) is almost twice σ_{π^-}(6-prongs), we normalize $\underline{F}$ and $\underline{G}$

to the cross section of each of the final states by defining $\Phi_{a(b)} = \frac{1}{2}(1 + \sigma_{b(a)}/\sigma_{a(b)})(F_{a(b)}/F_{total})$ and $\Gamma_{a(b)} = \frac{1}{2}(1 + \sigma_{b(a)}/\sigma_{a(b)}) \times (G_{a(b)}/G_{total})$ for final state a(b) (figs. 5a & 5d). Clearly, the shapes of these two distributions are identical.

Over the entire region of $p_\perp$ that we compare with D. Smith ($p_\perp < 0.7$ GeV/c) the 2π reaction always contributes less than $\frac{1}{2}G_{total}$ (only $\frac{1}{4}G_{total}$ at $p_\perp \gtrsim 0$); therefore, the 3π and even $\geq 4\pi$ events are important over the entire range of $p_\perp$ that we compare with higher energies.

Although final states having more π's fall off more rapidly with increasing x and $p_\perp$ than do final states with fewer π's, this effect is more pronounced for the x-distribution than for the $p_\perp^2$-distribution (table IV).

Table IV. Contributions of different final states to F and G when F_{total} and G_{total} have decreased one decade from their values at $x = 0$ and $p_\perp^2 = 0$, respectively

x-Distribution		$p_\perp^2$-Distribution	
$F_{2\pi}/F_{total}$	0.66	$G_{2\pi}/G_{total}$	0.42
$F_{3\pi}/F_{total}$	0.30	$G_{3\pi}/G_{total}$	0.42
$F_{\geq 4\pi}/F_{total}$	0.04	$G_{\geq 4\pi}/G_{total}$	0.16
$(x = 0.64)$		$(p_\perp^2 = 0.33\ (\text{GeV}/c)^2)$	

F. Two Dimensional Distributions

We now plot ρ for five equal intervals in $p_\perp$ from 0 to 1 GeV/c, against both x and the rapidity, y (fig. 6). Fig. 6 shows that ρ falls off more rapidly as x increases. Also, it appears that the initial fall-off of ρ with x is less rapid at higher values of $p_\perp$. In order to more clearly see any such differences in the shape of the ρ vs. x curves for different $p_\perp$, we plot R vs. $p_\perp$ for six intervals in x (fig. 6b), where $\underline{R}$ is defined by:

$$R(x,p_\perp,s) = \rho(x,p_\perp,s)/\rho(0,p_\perp,s).^\dagger \qquad (1)$$

The first two data points in $p_\perp$, for all $\underline{x}$, show a definite rise in $\underline{R}$ with $p_\perp$, a rise which generally becomes steeper with increasing $p_\perp$. The three curves representing the smallest $\underline{x}$ continue to rise, gradually flattening out, whereas the higher-$\underline{x}$ curves show a definite turnover before $p_\perp$ reaches its maximum value. The curves certainly are not flat. However, suppose that ρ could be factorized, i.e. suppose that we could write:

$$\rho(x,p_\perp,s) = g(x,s)h(p_\perp,s).$$

According to our definition of $\underline{R}$ (eqn. 1) we would then have:

$$R(x,p_\perp,s) = g(x,s)/g(0,s) = R(x,s).$$

Therefore, the observed dependence of $\underline{R}$ upon $p_\perp$ means that ρ is not factorizable for this data.

IV. DISCUSSION AND CONCLUSIONS

Feynman has chosen the C.M. system to be most appropiate for his parton-bremsstrahlung-model,[8] but Benecke, Chou, Yang, and Yen work in the lab. or beam rest frame, since these frames are most appropiate for their beam and target fragmentation picture.[9] Both models have been shown to be equivalent at high energy.[10]

Our experiment is clearly not at high energy, however. We have shown that only the laboratory distribution (for $x < -0.4$) is energy independant at our energy; the structure function ρ depends on energy when plotted against $\underline{x}$ or the rapididy difference $y - y_{min}$ or $y - y_{max}$. We note that some authors define $\underline{x}$ by $2p_\parallel^*/s^{\frac{1}{2}}$, $p_\parallel^*/p_o^*$ (p_o^* = the incident proton

---

†To be precise, $\underline{R}$ is the ratio of $\langle\rho\rangle_{av}$ for a bin in $p_\perp$ and $\underline{x}$, as defined above, divided by $\langle\rho\rangle_{av}$ for a bin with the same $p_\perp$ boundries and $\underline{x}$ running from 0.0 to 0.1.

momentum in the overall C.M. system), or $p^*_{\parallel}/p^*_{\parallel\,max}(p_\perp)$ [$p^*_{\parallel max}(p_\perp)$ = the maximum value of $p^*_{\parallel}$ for a given value of $p_\perp$]. We defined x as $p^*_{\parallel}/p^*_{max}$. We point out that these different definitions are far from identical at our energy, 6.6 GeV/c, although they become identical at large incident beam energy and not too large $p_\perp$. We chose $x = p^*_{\parallel}/p^*_{max}$ only because for

Table V. Different definitions of x

Definition of x	Value of x for identical values of $p^*_{\parallel}$ for P_{beam} = 6.6 GeV/c: $p^*_{\parallel} = p^*_{\parallel max}(p_\perp)$ for $p_\perp$ = 0.0	$p^*_{\parallel} = p^*_{\parallel\,max}(p_\perp)$ for $p_\perp$ = 0.5
$x = 2p^*_{\parallel}/s^{\frac{1}{2}}$	0.71	0.66
$x = p^*_{\parallel}/p^*_o$	0.82	0.76
$x = p^*_{\parallel}/p^*_{max}$ (our choice)	1.00	0.92
$x = p^*_{\parallel}/p^*_{\parallel\,max}(p_\perp)$	1.00	1.00

this definition the maximum value of x is energy independant, and because this definition does not mix events of different $p^*_{\parallel}$ according to $p_\perp$.

We have also seen that ρ does not factorize, i.e. $\rho(x,p_\perp,s) \neq g(x,s) \chi h(p_\perp,s)$.

ACKNOWLEDGMENTS

I wish to express my appreciation to my collaborators in this 1965 experiment: William M. Dunwoodie (now of CERN TC Division), Eugene Paul Colton (now of LBL), Peter Schlein, and Harold K. Ticho, all from UCLA; and Robert J. Manning, Gerald A. Smith (now of MSU), Arthur Barry Wicklund (now of ANL), and Stanley Wojcicki (now of SLAC), all from the Lawrence Berkeley Laboratory.

I also wish to thank Clifford Risk for his very helpful discussions on

the subject of inclusive reactions, including his suggestions for some of the plots contained herein.

This work has been supported by the United States Atomic Energy Commission.

REFERENCES

1. (a). Eugene Paul Colton, Pion Production in Proton-Proton Interactions at 6.6 GeV/c (Ph. D. Thesis), UCLA-1025, June 1968; and (b). William M. Dunwoodie, Strange Particle Production in Proton-Proton Interactions at 5.4 and 6.6 GeV/c (Ph. D. Thesis), UCLA-1033, Dec. 1968

2. M.A. Abolins, G. A. Smith, Z. Ming Ma, Eugene Gellert, and A. B. Wicklund, Phys. Rev. Lett. 25, 126 (1970)

3. F. T. Solmitz, A. D. Johnson, and T. B. Day, Three View Geometry Program (TVGP), Lawrence Berkeley Laboratory - Group A programming note P-117, June 1965; O. I. Dahl, T. B. Day, and F. T. Solmitz, SQUAW - Kinematic Fitting Program, Lawrence Berkeley Laboratory - Group A programming note P-126, August 1965

4. Dennis Baird Smith, Charged Pion Production in Proton-Proton Interactions Between 13 and 28.5 GeV/c (Ph. D. Thesis), Lawrence Berkeley Laboratory UCRL-20632, March 1971

5. Dennis Baird Smith (Orsay), personal communication, 1971

6. Akerlof et al., Phys. Rev. D3, 645 (1971)

7. Eugene Colton and Alan Kirschbaum, Study of $|T_z| = 3/2\ \Delta(1238)$ Production in pp Interactions at 6.6 GeV/c, Lawrence Berkeley Laboratory LBL-730, Feb. 1972 (to be submitted to Phys. Rev.)

8. Richard P. Feynman, The Behavior of Hadron Collisions at Extreme Energies, in High Energy Collisions / Third International Conference / Stony Brook, 1969, edited by C. N. Yang and others, (Gordon & Breach, New York, 1969); Richard P. Feynman, Phys. Rev. Lett. 23, 1415 (1969)

9. J. Benecke, T. T. Chou, C. N. Yang, and E. Yen, Phys. Rev. 188, 2159 (1969)

10. J. C. Vander Velde, Phys. Lett. 32B, 501 (1970)

ADDENDUM

In addition to the plot of ρ vs. $\underline{x}$ discussed in the main text (fig. 2b), we also plot ρ against three other definitions of $\underline{x}$ (fig. 7). (Refer to table V and the nearby text for a discussion of the different definitions of $\underline{x}$.) Fig. 7b shows agreement for $x_2 \gtrsim 0.4$ (where $x_2 = p^*_{//}/P^*_0$, and P^*_0 is the momentum of the incident proton in the C.M. system) and $p_\perp^2 = 0.21\ (\mathrm{GeV}/c)^2$ (except possibly for the two points highest in x_2), unlike the ρ vs. x_3 plot (figs. 2b and 7c). It therefore seems that x_2 is a better scaling variable than x_3 (where $x_3 = p^*_{//}/p^*_{max}$). However, comparisons at other (lower) values of $p_\perp$ must be made before one can be certain of this.

FIGURE CAPTIONS

Fig. 1. $d^2\sigma/dp_\perp dp_\parallel$ vs. $p_\parallel(\mathrm{lab})_{\pi^-}$ for 7 different intervals in $p_\perp$ from 0 to 0.7 GeV/c. The open circles (○) are D. Smiths's data from 13 to 28.5 GeV/c taken from ref. 4, and the solid circles (●) are from this experiment. The three pairs of solid lines delimit (1) the lower kinematic limit of $p_\parallel$(lab), and (2) and (3), the regions where it is possible to have $\underline{x} = -0.5$ and $\underline{x} = 0$, respectively, for the 6.6 GeV/c data. The broken lines delimit the same regions for the 13 to 28.5 GeV/c data. (Some of these lines lie beyond the plot boundries, and are therefore not drawn.)

Fig. 2 Comparison of 6.6 GeV/c data (this experiment) with 12.4 GeV/c data (Akerlof et al. - ref. 6) for $p_\perp^2 = 0.21$, 0.41, & 1.03 $(\mathrm{GeV/c})^2$. (For fig. 2b, our points are averaged over bins centered on Akerlof et al.'s values of both $\underline{x}$ and $p_\perp^2$, and with bin widths Δx = difference in $\underline{x}$ between Akerlof's points, and $\Delta p_\perp^2 = 0.1\ (\mathrm{GeV/c})^2$. All the other plots are obtained by transforming the fig. 2b points.) A broken line joins points having $|x| = 0.489$ ($x = p^*_\parallel/p^*_{max}$ - Feynamn's $\underline{x}$), except for fig. 2c.

a. $d^2\sigma/dp_\perp dp_\parallel$ vs. $p_\parallel(\mathrm{lab})_{\pi^-}$

b. ρ vs. x ($\rho = Ed^3\sigma/dp^3$, $x = p^*_\parallel/p^*_{max}$)

c. $(1/\sigma_{\pi^-})d^2\sigma/dp_\perp^2 dp^*_\parallel$ vs. $p^*_\parallel$ ("*" means a C.M. variable)

d. ρ vs. $\underline{y}$ (the π^- lab. rapidity, $y = \tanh^{-1}(p_\parallel/E)$)

Fig. 3. Longitudinal distributions for π^-'s from $pp \to \pi^-$ + anything at 6.6 GeV/c. The upper curve of each plot (□) is the combined 4 and 6-prong sample, whereas the lower two curves of each plot (-) are the 4 and 6-prong samples respectively. The error bars represent statistical errors only. The error bars for the combined data do not include the effect of the ± 12% uncertainty in the cross-section ratio σ_6/σ_4, which causes a maximum error of ± 2% in the combined data. The overall normalization error of ≈ 5% is not shown. (On those plots where it is shown, point $\underline{a}$ is a typical 6-prong data point with a ± 12% error, and point $\underline{b}$ is a typical combined data point with a ± 2% error.)

a. $F(x,s)$ vs. x, where $F(x,s) = \int_0^{p^2_{\perp,max}} \rho(x,p_\perp^2,s)dp_\perp^2$ and $x = p^*_\parallel/p^*_{max}$ ($\rho = Ed^3/dp^3$)

b. $d\sigma/dx$ vs. x

c. $d\sigma/dp_\parallel$ vs. $p_\parallel$(lab)

d. $B(y,s)$ vs. y, where $B(y,s) = \int_0^{p^2,max} \rho(y,p_\perp^2,s)dp_\perp^2$, and the rapidity, $y \doteq \tanh^{-1}(p/E)$

Fig. 4. Spectra for 2π, 3π, and $\geq 4\pi$ final states (as well as all final states) for $pp \to \pi^-$ + anything at 6.6 GeV/c.

a. $F(x,s)$ vs. $\underline{x}$

b. $G(p_\perp^2,s)$ vs. $p_\perp^2$, where $G = \int_{-1}^{+1} \rho(x,p_\perp^2,s)dx$

Fig. 5. Fractional contributions of various final states to $\underline{F}$ and $\underline{G}$ (see fig. 3 & 4 captions for definitions of $\underline{F}$ and $\underline{G}$.) for $pp \rightarrow \pi^- +$ anything at 6.6 GeV/c.

a. F/F_{total} vs. $\underline{x}$ for the two 3π final states: $pp\pi^+\pi^-\pi^o$ and $pn\pi^+\pi^+\pi^-$

b. $\bar{\Phi}$ vs. x for the two contributions to $\geq 4\pi$ final states: 4-prongs ($\geq 4\pi$ only) and 6-prongs (all are $\geq 4\pi$). (See text for details.)

c. F/F_{total} vs. x for 2π, 3π, and $\geq 4\pi$ final states

d. G/G_{total} vs. $p_\perp^2$ for the two 3π final states; $pp\pi^+\pi^-\pi^o$ and $pn\pi^+\pi^+\pi^-$

e. Γ vs. $p_\perp^2$ for the two contributions to $\geq 4\pi$ final states: 4-prongs ($\geq 4\pi$ only) and 6-prongs (all are $\geq 4\pi$) (see text)

f. G/G_{total} vs $p_\perp^2$ for 2π, 3π, and $\geq 4\pi$ final states

Fig. 6. Two dimensional spectra - ρ_{π^-} - from $pp \rightarrow \pi^- +$ anything at 6.6 GeV/c

a. ρ vs. $\underline{x}$ for 5 intervals in $p_\perp$

b. $R(x,p_\perp,s)$ vs. $p_\perp$ for 6 intervals in $\underline{x}$, where $R(x,p_\perp,s) = \rho(x,p_\perp,s)/\rho(0,p_\perp,s)$. For $\rho(x=0)$ we actually use $\langle\rho(x=0-0.1)\rangle_{av}$. The symbols with horizontal error bars are not data points, but represent $p_{\perp,max}$ for each x-interval. [The low end of each error bar is $p_{\perp,max}$ for the highest $\underline{x}$ in the x-interval.]

c. ρ vs. y for 5 intervals in $p_\perp$ (the lab. rapidity $y = \tanh^{-1}(p_\parallel/E)$)

Fig. 7 ρ vs. $\underline{x}$ for $pp \rightarrow \pi^- +$ anything at 6.6 GeV/c (this experiment) and 12.4 GeV/c (Akerlof $\underline{et\ al}$.- ref. 6) for four different definitions of $\underline{x}$. (See fig. 2 caption for more details.)

a. ρ vs. x_1 ($x_1 = 2p^*_\parallel/s^{\frac{1}{2}}$)

b. ρ vs. x_2 ($x_2 = p^*_\parallel/P^*_o$, P^*_o = C.M. momentum of the incident proton)

c. ρ vs. x_3 ($x_3 = p^*_\parallel/p^*_{max}$ - the same as fig. 2b)

d. ρ vs. x_4 ($x_4 = p^*_\parallel/p^*_{\parallel,max}(p_\perp)$)

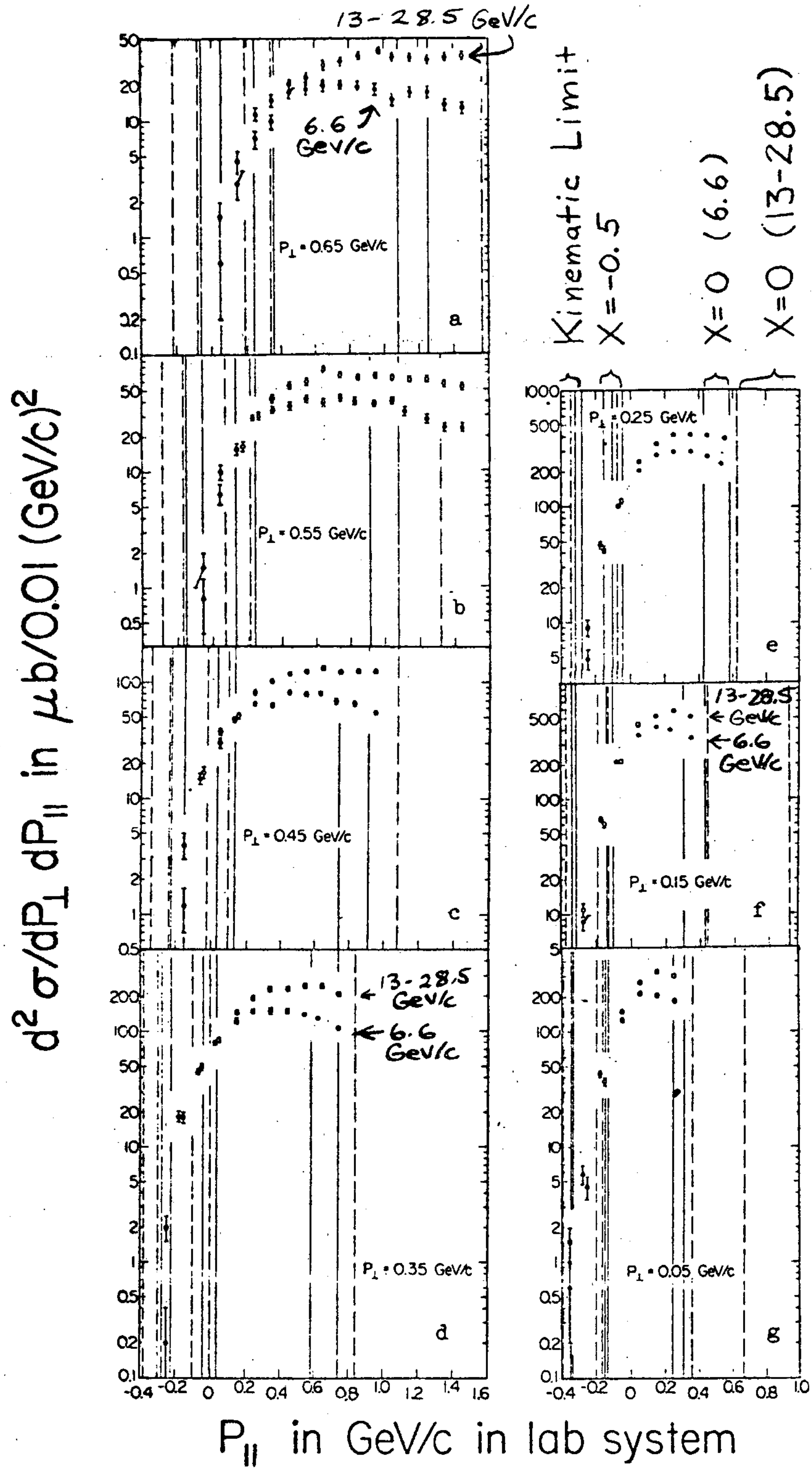

Fig. 1

XBL 722-286

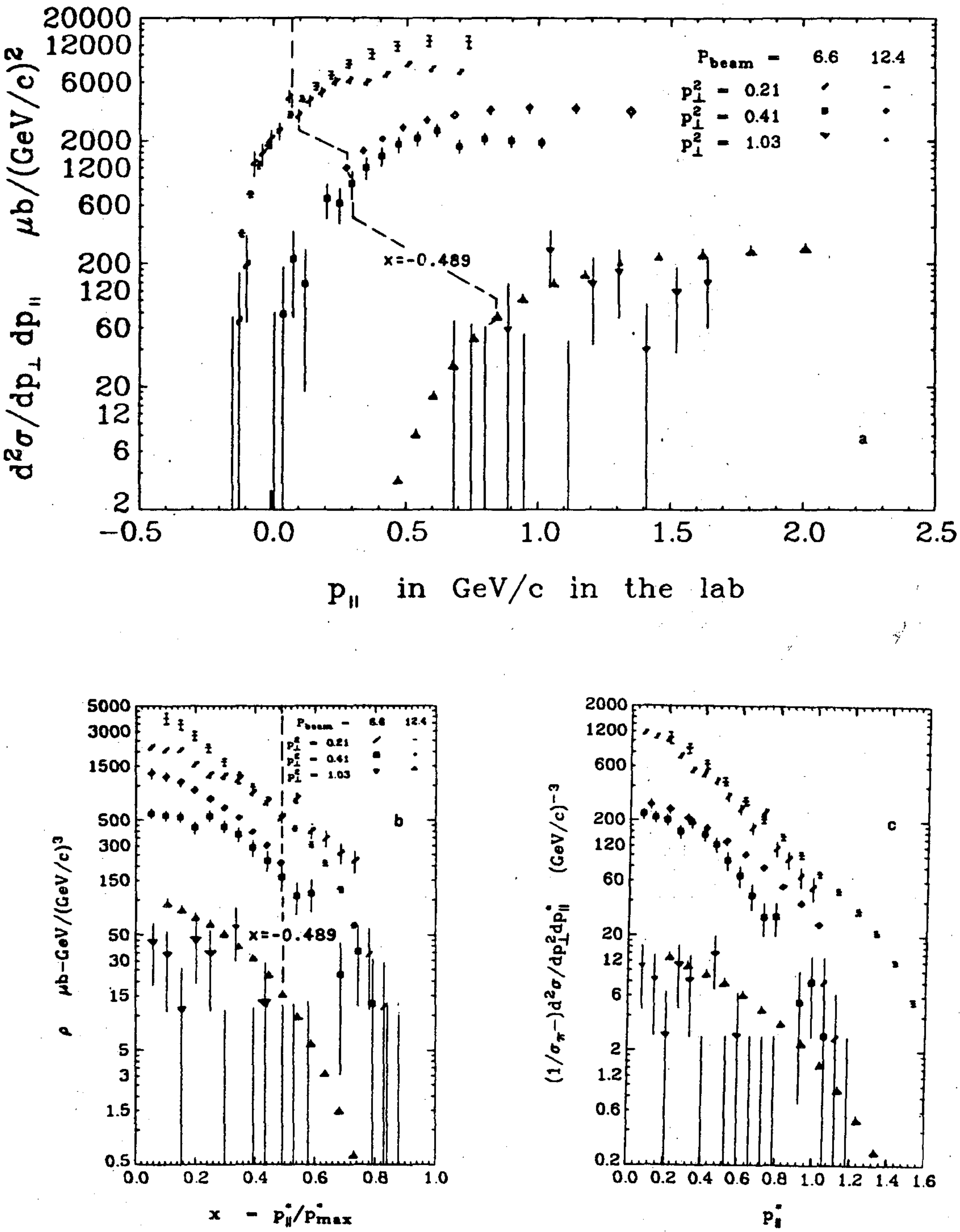

Fig. 2 (a,b,c)

XBL 724-742

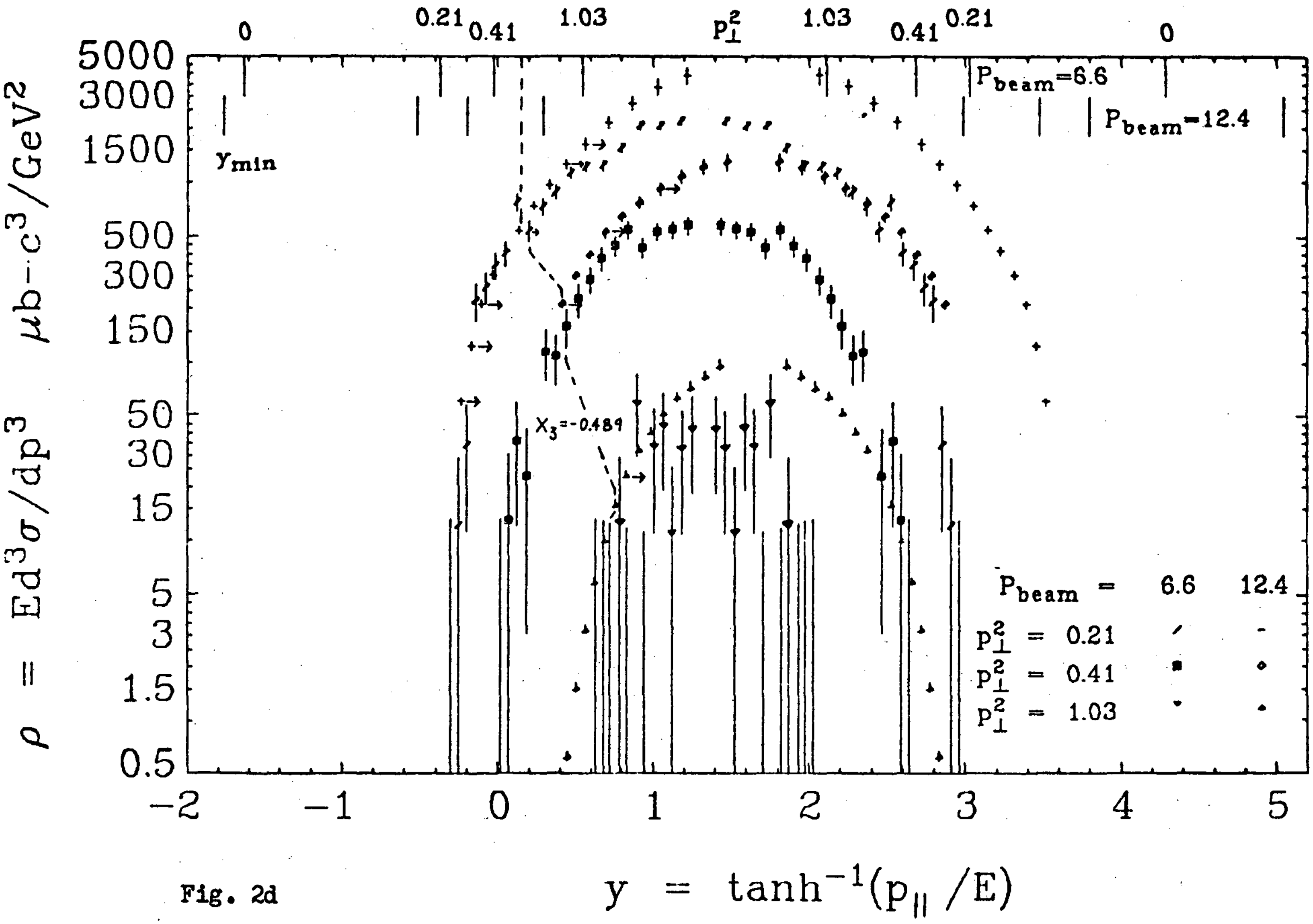

Fig. 2d

XBL 722-117

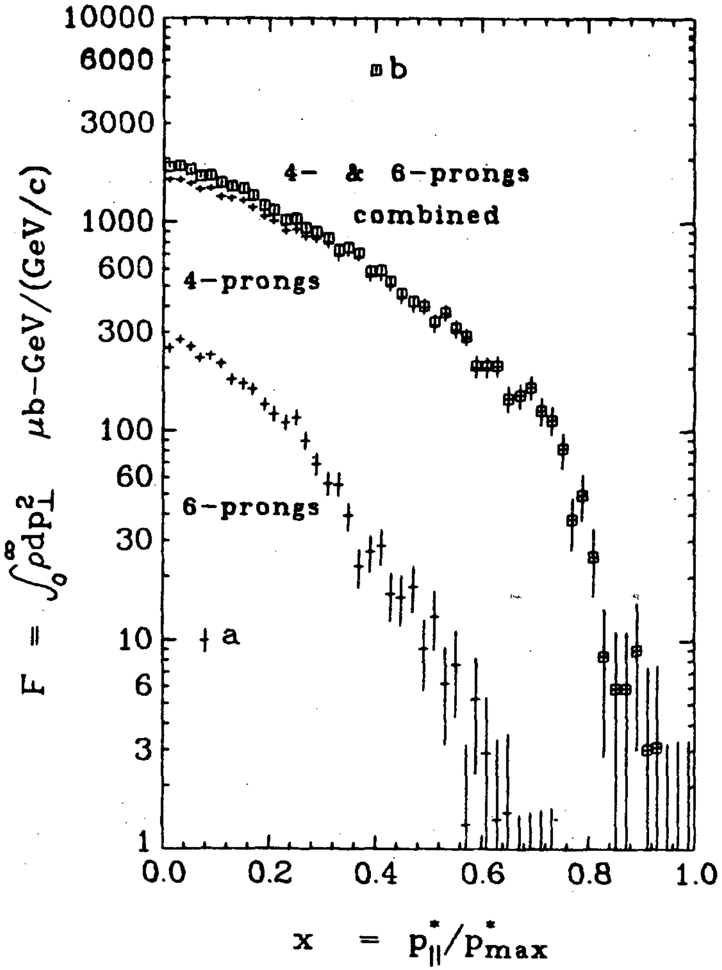

Fig. 3a

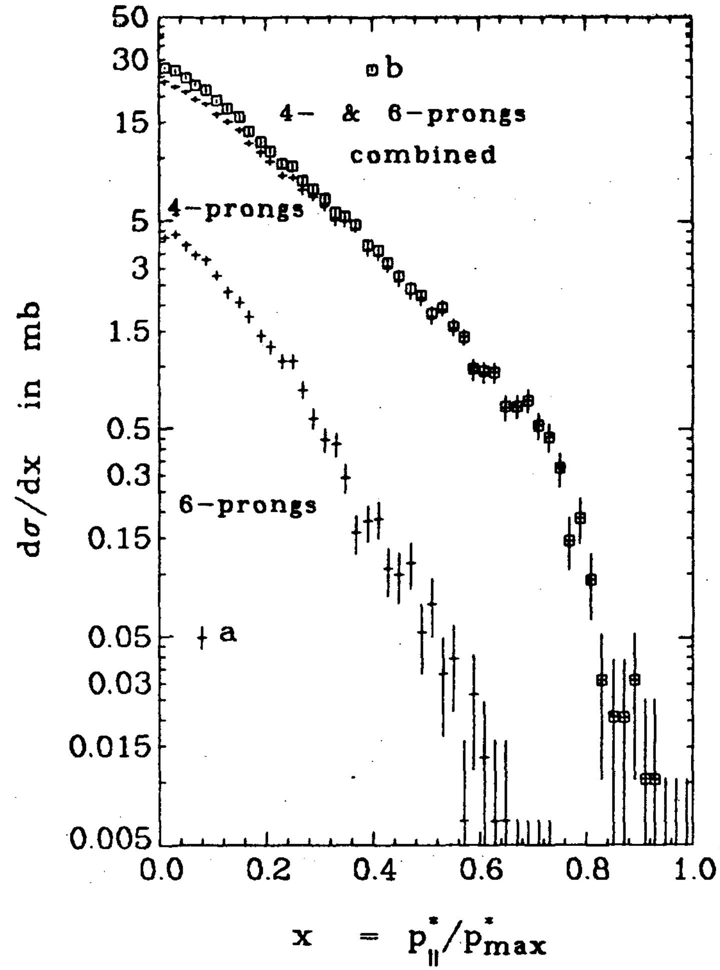

Fig. 3b

XBL 724-739

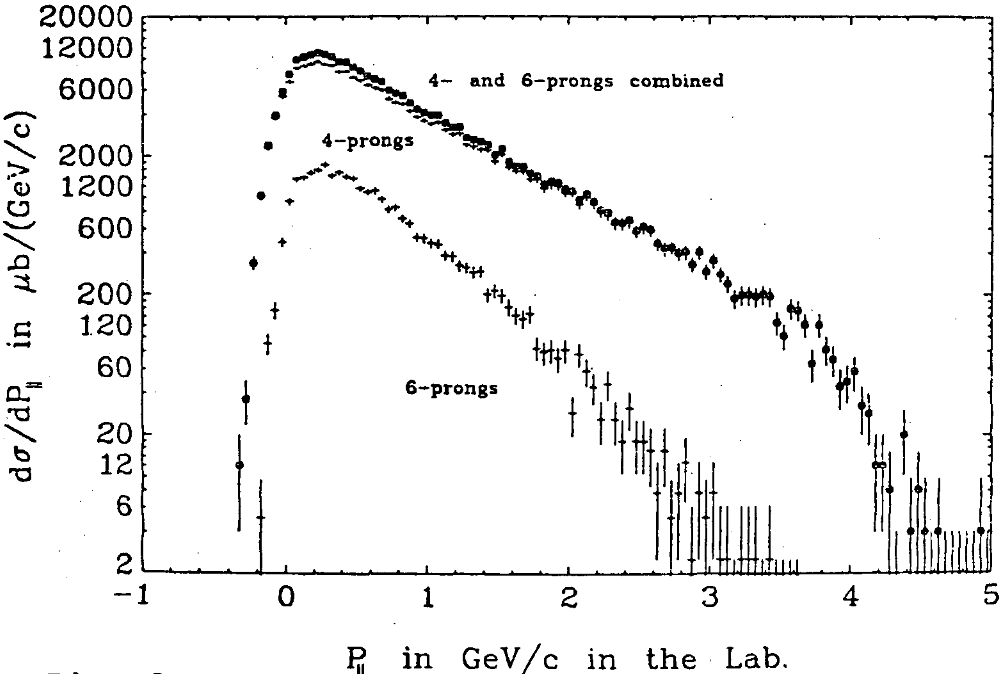

Fig. 3c

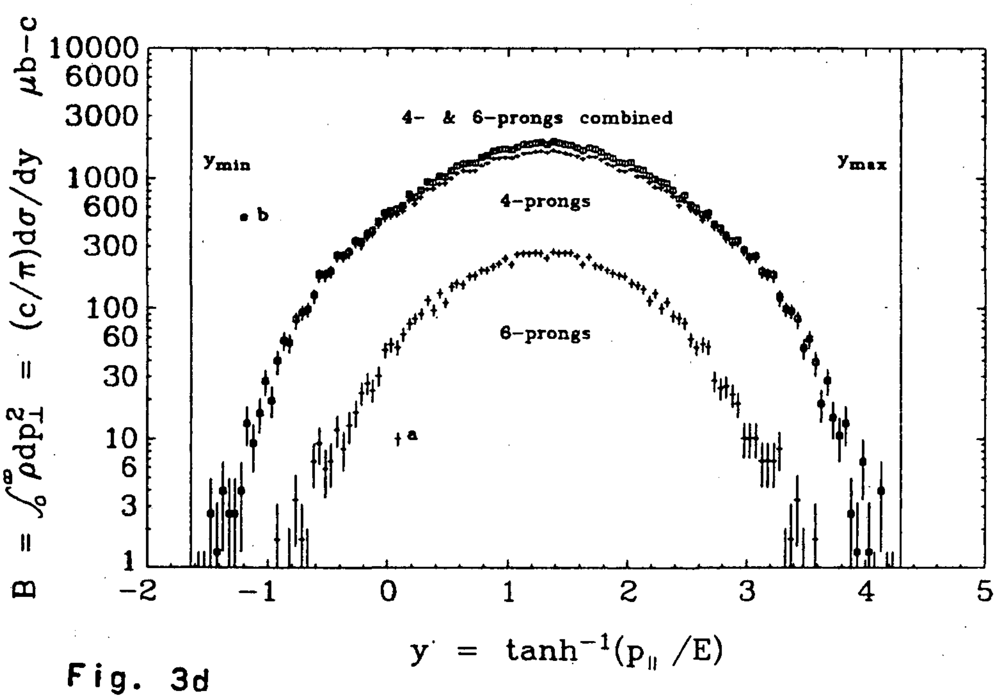

Fig. 3d

XBL 724-740

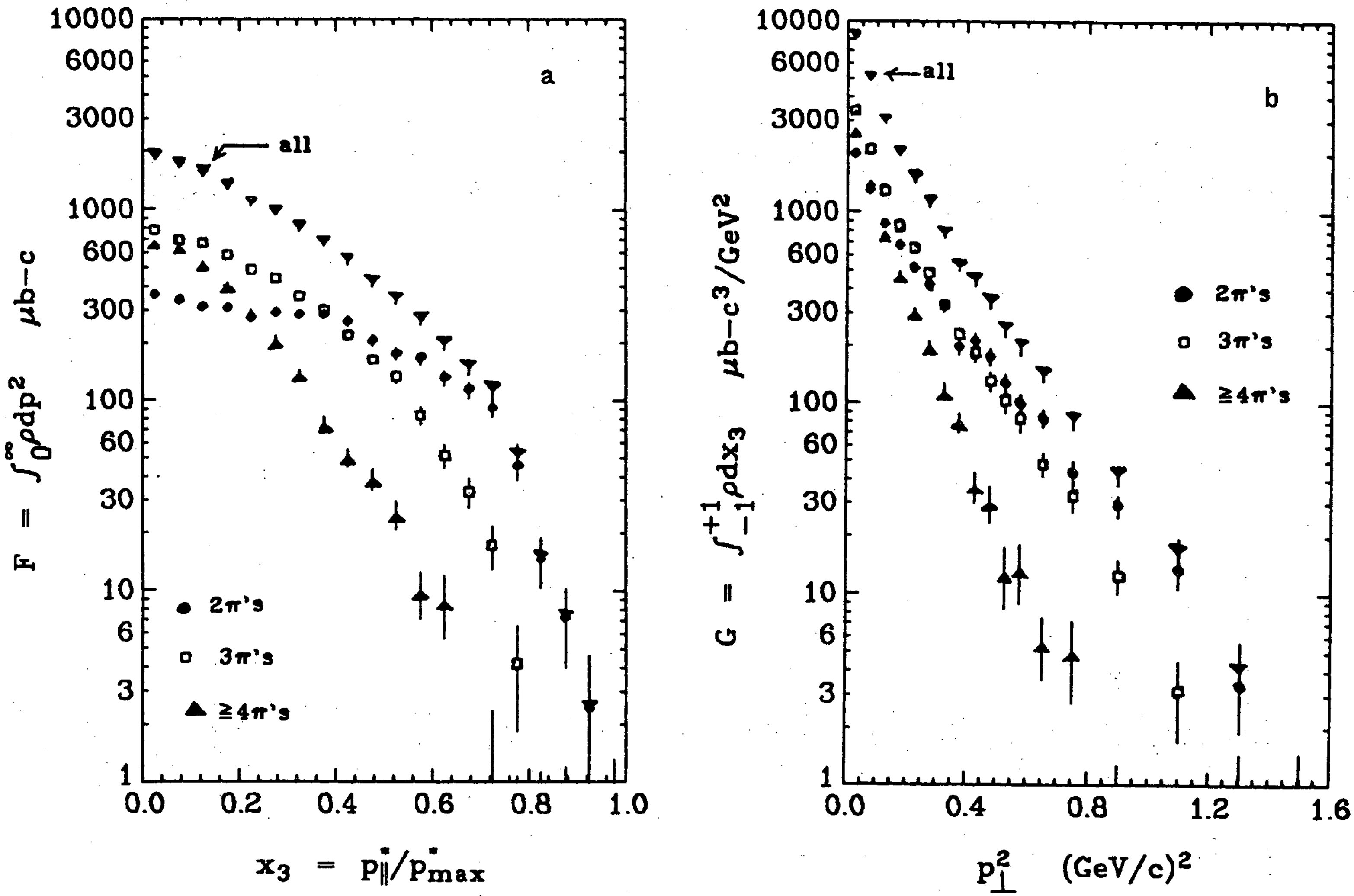

Fig. 4

XBL 724-737

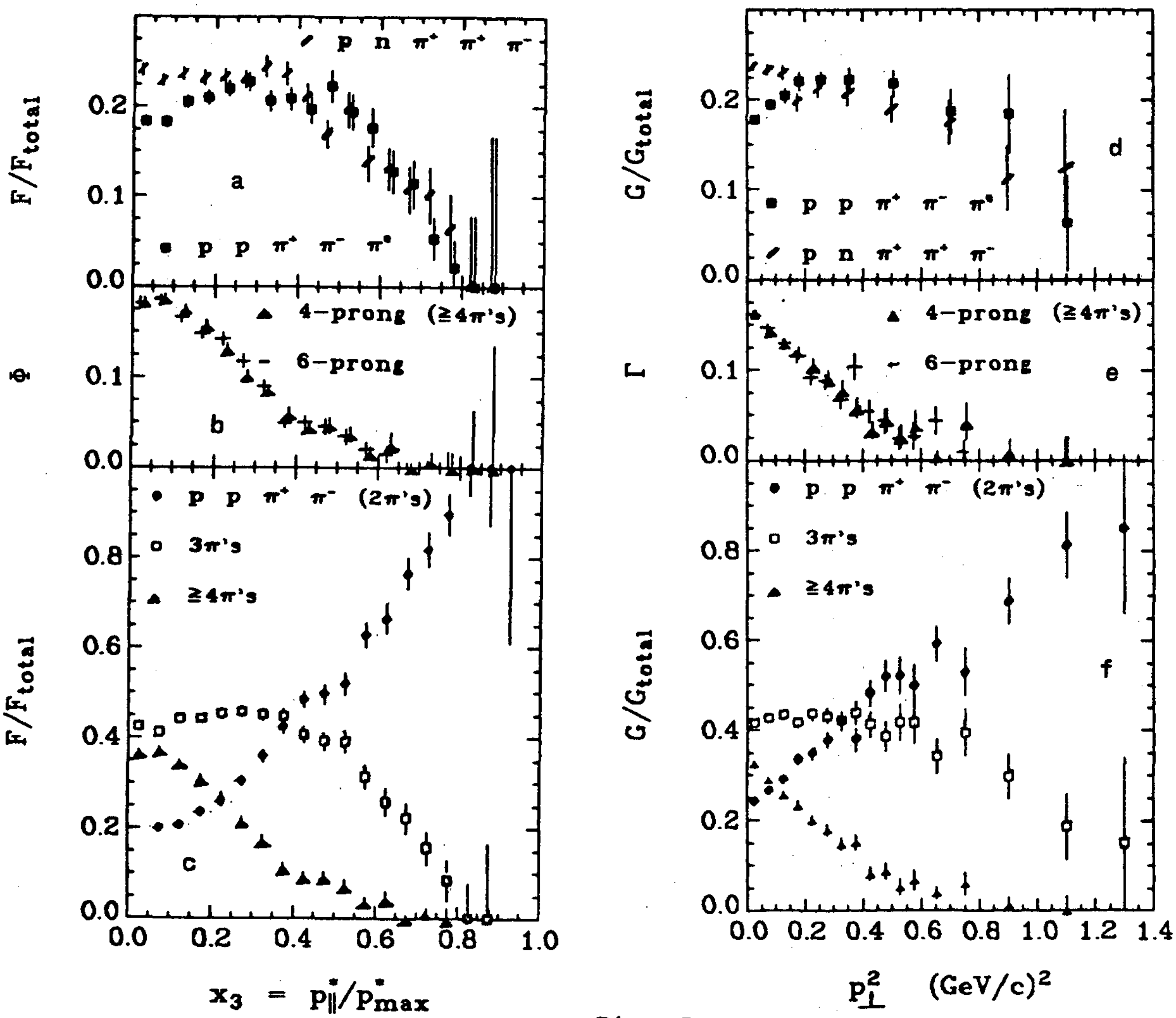

Fig. 5

XBL 724-738

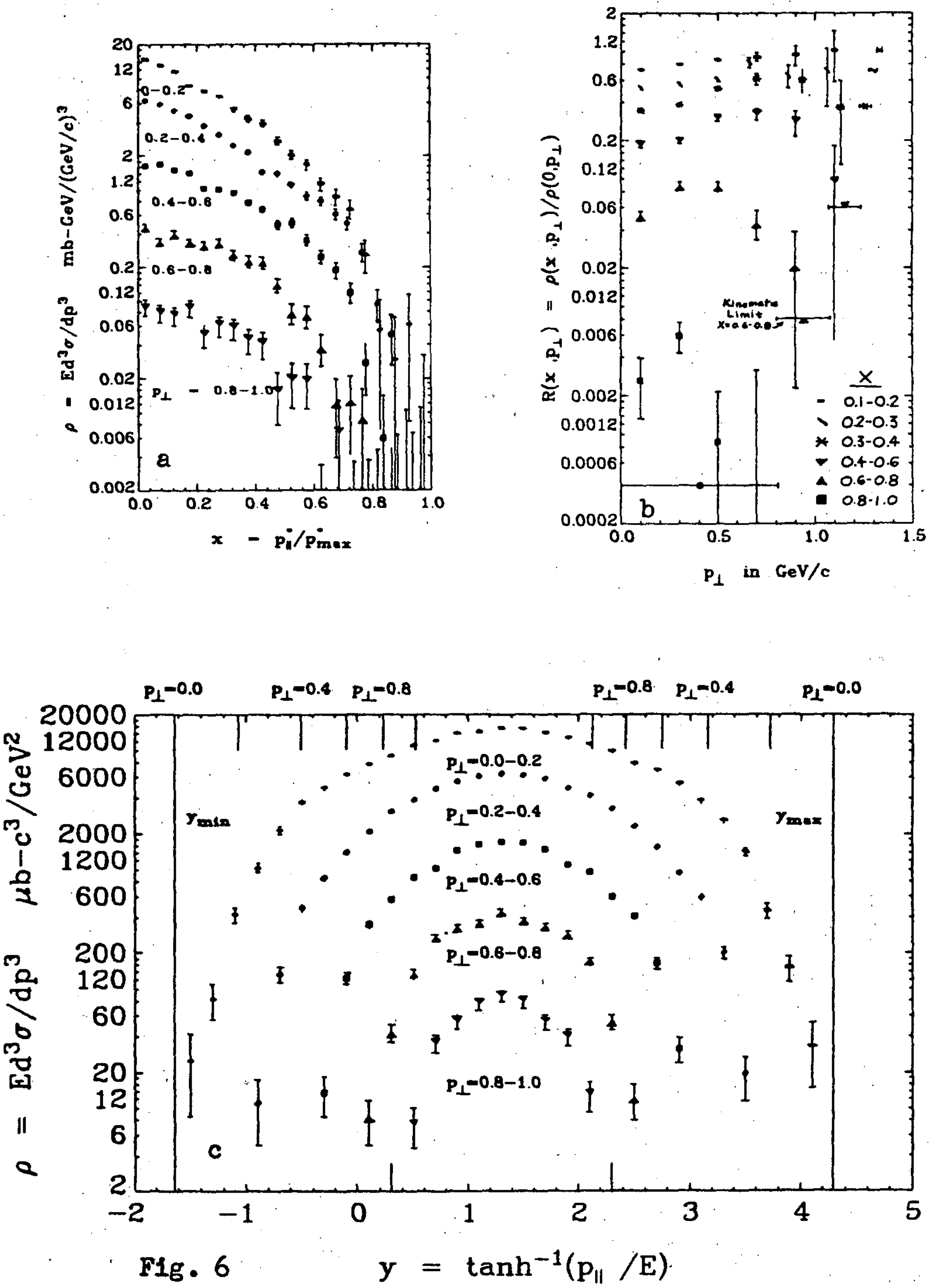

Fig. 6

XBL 724-741

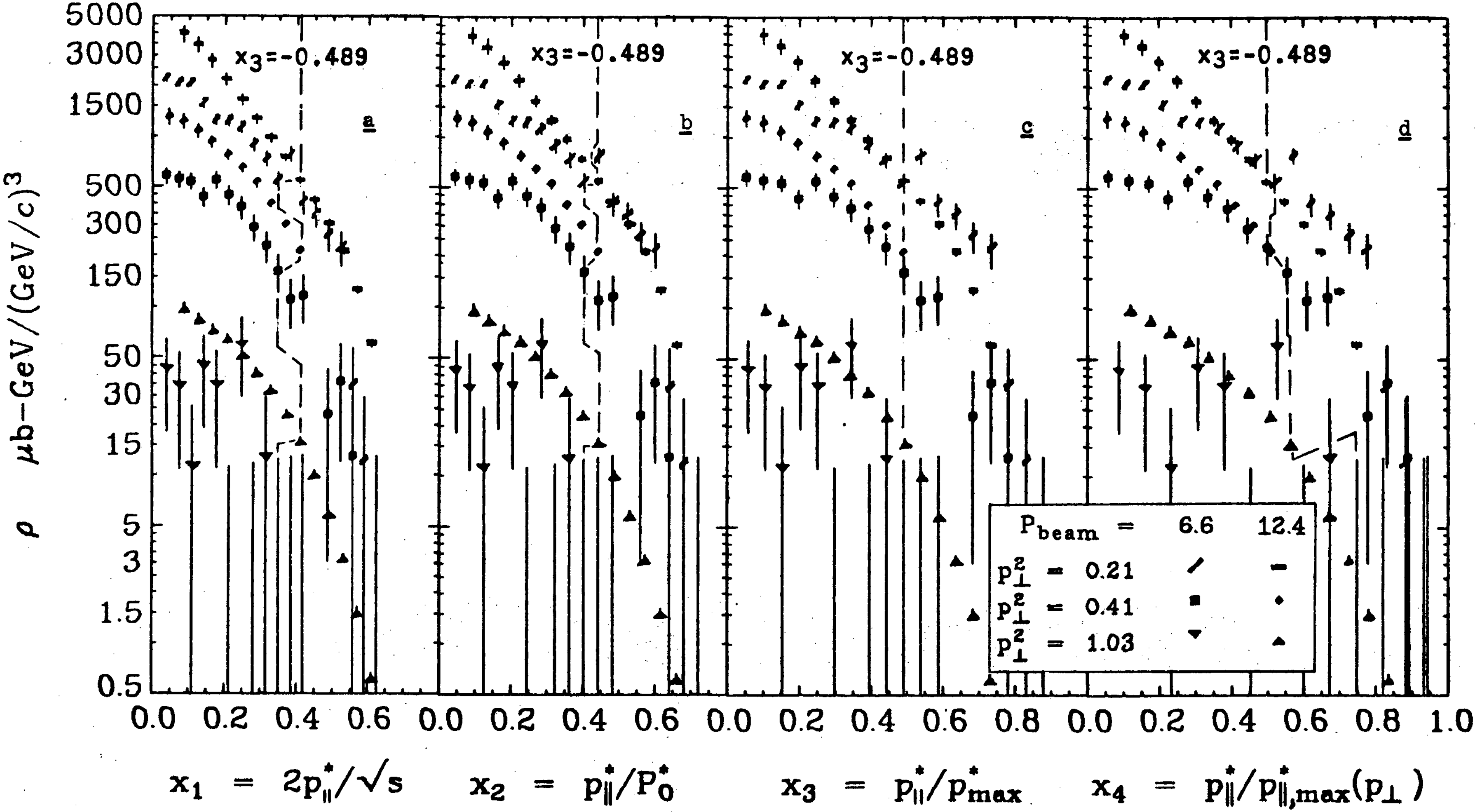

ρ μb-GeV/(GeV/c)^3
5000
3000
1500
500
300
150
50
30
15
5
3
1.5
0.5
x3=-0.489
a
b
c
d
P beam = 6.6 12.4
p⊥² = 0.21
p⊥² = 0.41
p⊥² = 1.03
0.0 0.2 0.4 0.6
0.0 0.2 0.4 0.6
0.0 0.2 0.4 0.6 0.8
0.0 0.2 0.4 0.6 0.8 1.0
x1 = 2p∥*/√s
x2 = p∥*/P0*
x3 = p∥*/p*max
x4 = p∥*/p∥,max*(p⊥)

Fig. 7

TECHNICAL INFORMATION DIVISION
LAWRENCE BERKELEY LABORATORY
UNIVERSITY OF CALIFORNIA
BERKELEY, CALIFORNIA 94720